Earth and Planetary Science Letters 307 (2011) 180–190

Contents lists available at ScienceDirect

Earth and Planetary Science Letters

journal homepage: www.elsevier.com/locate/epsl

Links between orogenic wedge deformation and erosional exhumation: Evidence from illite age analysis of fault rock and detrital thermochronology of syn-tectonic conglomerates in the Spanish Pyrenees

Jeffrey M. Rahl [a,*], Samuel H. Haines [b,1], Ben A. van der Pluijm [b]

[a] Department of Geology, Washington and Lee University, Lexington, VA, 24450, USA
[b] Department of Geological Sciences, University of Michigan, Ann Arbor, MI, 48109, USA

ARTICLE INFO

Article history:
Received 23 October 2010
Received in revised form 23 April 2011
Accepted 26 April 2011
Available online 19 May 2011

Editor: T.M. Harrison

Keywords:
Clay gouge
detrital thermochronology
Argon–Argon dating
Pyrenees
orogenic wedge

ABSTRACT

We present new geochronologic data illuminating the tectonic and erosional history of the orogenic wedge exposed in the south-central Pyrenees, Spain. We interpret illite-age analyses from four fault gouges that record thrust-belt development and document the importance of out-of-sequence thrusting. Fault activity occurs in pulses, with slip occurring contemporaneously on multiple faults throughout the wedge. New apatite fission-track data from syn-orogenic sediments of the Sis Conglomerate body reveal ages of 48 to 42 Ma, with no consistent variation upsection in strata deposited from 41 to 30 Ma. We interpret these data, as well as thermal modeling of track-length distributions, to imply rapid cooling in the interior of the Pyrenean wedge during the Middle Eocene. The record of fault activity and erosion suggests that orogenic wedges may not evolve in a steady fashion, but generally exhibit significant changes in rates of deformation and exhumation. The observed correlation in the timing of tectonism and erosional exhumation provides evidence for links between tectonic and surface processes.

1. Introduction

As links between tectonic and climatic forces are increasingly well-documented, erosion has been recognized as a key parameter impacting the long-term evolution of orogenic belts (e.g., Dahlen and Suppe, 1988). Patterns and rates of erosion affect fundamental aspects of mountain building, including the development of surface topography and relief, orogen size and width (Roe et al., 2006; Stolar et al., 2006; Whipple and Meade, 2004), and the flow of crustal material within an orogen (Willett, 1999). Of key importance is the relationship between erosion and crustal deformation. Both numerical and analogue models demonstrate that the pattern of erosion in mountain belts exerts a major control on the structural evolution of orogenic wedges (e.g., Beaumont et al., 1992; Konstantinovskaia and Malavieille, 2005; Koons, 1990; Willett, 1999). In order to test and refine our understanding of these processes, it is essential to study records of deformation and erosion in natural settings.

Our goal is to investigate the relationship between deformation and erosional exhumation in the central Spanish Pyrenees. Previous work provides a relatively detailed history of faulting in the frontal fold-thrust belt (Burbank et al., 1992b; Meigs, 1997; Meigs et al., 1996), and the record of bedrock exhumation in the interior of the mountain belt is documented through several thermochronology studies (Fitzgerald et al., 1999; Gibson et al., 2007; Metcalf et al., 2009; Sinclair et al., 2005). In this contribution, we expand and refine these records, presenting $^{40}Ar/^{39}Ar$ data from fault gouge that provide absolute ages of motion on Pyrenean thrusts. Several of these results focus on structures in the interior of the orogen, where stratigraphic approaches to bracketing episodes of slip are limited. We also describe new detrital apatite fission-track ages that complement the record of Pyrenean exhumation from bedrock cooling data. The data presented here enable us to address key questions about the tectonic and erosional evolution of wedges with time. Does within-wedge deformation evolve in a relatively simple fashion, with active faults progressively migrating toward the foreland, or do out-of-sequence thrusts play an important role? Do the previously documented changes erosion of the wedge interior correspond to variations in tectonic activity? Our data demonstrate the significance of out-of-sequence faulting and suggest a relationship between tectonic and surface processes, with episodes of faulting coincident with periods of accelerated erosional exhumation of the Pyrenean wedge.

* Corresponding author. Tel.: +1 540 458 8101.
E-mail address: rahlj@wlu.edu (J.M. Rahl).
[1] Now at: Chevron Energy Technology Corporation, 1500 Louisiana Street, Houston, TX, 77002, USA.

0012-821X/$ – see front matter © 2011 Elsevier B.V. All rights reserved.
doi:10.1016/j.epsl.2011.04.036

2. Geologic background

The Pyrenean mountain chain stretches for ~1500 km, the result of continental collision between the European and Iberian Plates. Late Cretaceous through Early Miocene convergence involved at least 165 km of shortening, with Iberian lithosphere thrust a minimum of 80 km beneath Europe (Beaumont et al., 2000; Choukroune et al., 1989; Ledo et al., 2000; Muñoz, 1992; Souriau and Granet, 1995). The orogen is an excellent example of an asymmetric, doubly-vergent wedge. To the north, the retro-wedge comprises imbricated Mesozoic cover and basement derived from the European Plate and separated from more southerly Iberian rocks by the strike-slip North Pyrenean Fault (Fischer, 1984). On the pro-side of the orogen, south-verging imbricate thrust sheets expose Mesozoic platform carbonates and Paleogene siliciclastics. Syn-deformational sediments preserved throughout the fold-thrust belt have enabled an unusually detailed reconstruction of pro-wedge evolution, with deformation from ~55–25 Ma characterized by changes in the slip-rates and position of active thrusts (e.g., Burbank et al., 1992b; Deramond et al., 1993; Meigs et al., 1996; Meigs and Burbank, 1997; Williams et al., 1998).

The core of the mountain belt, the Axial Zone, exposes the most deeply exhumed rocks, a series of pre-Cambrian through Carboniferous basement thrust sheets initially stacked during Hercynian orogenesis (Muñoz, 1992; Zwart, 1986). Structural and petrologic observations suggest that these sheets were intruded syntectonically by crustal-derived granodioritic plutons around 300 Ma (Evans et al., 1998). Subsequent deformation warped these units into the broad, south-vergent antiformal stack observed in the modern cross-section (Beaumont et al., 2000; Muñoz, 1992; Seguret and Daignieres, 1986).

Structural and metamorphic data suggest about 15 km of exhumation has occurred in the core of the Axial Zone (Muñoz, 1992). Erosion is inferred to be the primary exhumation process in the interior of the belt because of a lack of field evidence for normal faulting or tectonic thinning. Apatite fission-track and other thermochronologic data document the history of erosion in the Axial Zone (Fitzgerald et al., 1999; Metcalf et al., 2009; Sinclair et al., 2005). Near-vertical age-elevation profiles obtained from several massifs throughout the central Pyrenees document both spatial and temporal variations in exhumation throughout the mountain belt. For example, the age-elevation profile from the Maledeta Massif shows an upper portion with invariant ages and long fission-track-length distributions, suggesting an episode of rapid cooling around 32 Ma (Fitzgerald et al., 1999). Lower elevations in this transect yield younger ages, defining a shallow slope that indicates a significant deceleration in cooling rate. Comparisons with other vertical transects, both to the north and south of the Maledeta region, reveal a general pattern of younging to the south (Fitzgerald et al., 1999; Sinclair et al., 2005), with apatite fission-track ages as young as 20 Ma. Sinclair et al. (2005) interpreted this pattern of ages to reflect a shift in the position of maximum erosion caused by progressive southward growth of the Pyrenean wedge.

Much of the material eroded from the interior of the orogen was transported to the foreland and deposited in the Ebro Foreland Basin and smaller wedge-top basins in the fold-thrust belt. The Ebro Basin sediments record a transition from initial marine sedimentation (turbidites, carbonates) to more continental deposits, with deltaic, fluvial, alluvial, and occasional lacustrine sediments dominant by late Miocene (e.g., Puigdefàbregas et al., 1992). Noteworthy is a thick package (up to 3 km) of fluvial–alluvial sediments that buried the growing fold-thrust belt during the Eocene–Oligocene (Coney et al., 1996), stabilizing the thrust wedge (Sinclair et al., 2005).

Central to our study are the Sis conglomerates (Vincent, 2001), preserved in a 20 km by 7 km body that contains over 1400 m of sediment deposited from the Middle Eocene to Oligocene. Vincent and Elliott (1997) interpreted these fluvial–alluvial sediments to represent deposition in a northeast–southwest trending paleovalley that served as a major conduit for eroded material to be transported to the Ebro Basin. Clast composition in the Sis conglomerates generally is dominated by Mesozoic carbonates and Paleozoic metasediments derived from lower thrust sheets of the Axial Zone, but also present locally throughout the section are cobbles of Hercynian granitoid. As described below, apatite fission-track dating of these clasts provides a means to track the history of erosional exhumation in interior of the Pyrenees.

3. Methods

3.1. Illite age analysis of fault gouge

The timing of fault slip in fold-thrust belts is usually estimated by establishing the age of events that preceded and followed fault motion

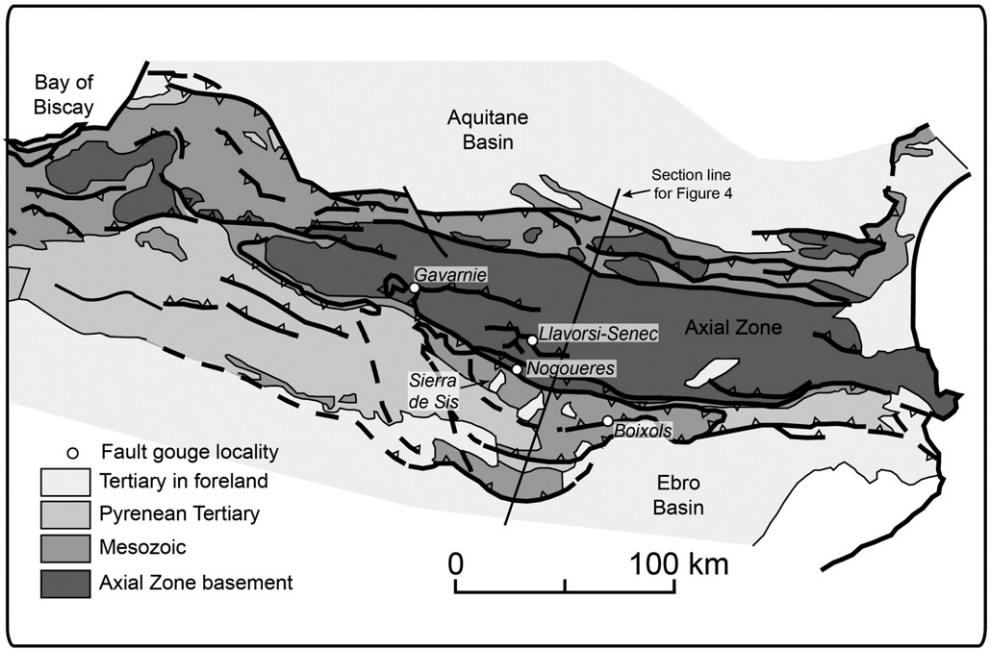

Fig. 1. Simplified geologic map of the Pyrenees, with fault-gouge sample localities.

(e.g., Armstrong and Oriel, 1965; Farrell et al., 1985; Puigdefàbregas and Souquet, 1986; Williams, 1985) or by dating syn-tectonic sediments using biostratigraphic or paleomagnetic techniques (e.g., Burbank et al., 1992a,b; Meigs, 1997; Meigs et al., 1996; Sussman et al., 2004). Dependent upon the local geology, these approaches are commonly inapplicable or may provide only loose ages. Recent work has demonstrated that the direct dating of authigenic clay mineralization in clay-rich fault gouges provides a reliable alternative to establish the timing of slip on brittle faults (Solum et al., 2005; van der Pluijm et al., 2001; van der Pluijm et al., 2006; Ylagan et al., 2002). Growth of authigenic minerals, particularly the 1 M/1M_d polytype of illite (mixed-layer illite-smectite), is a key process in the development of clay-rich gouges at temperatures less than 180 °C (Grathoff et al., 2001; Vrolijk and van der Pluijm, 1999). Typical fault gouge also contains the 2M_1 polytype of illite, a higher temperature (>280 °C, Srodon and Eberl, 1984) phase commonly inherited from the surrounding wallrock. Therefore, the measured $^{40}Ar/^{39}Ar$ age of a gouge samples will be a mixture of the ages of the detrital and authigenic components. The detrital component represents the age of grains mechanically introduced into the gouge from the host rock. If the wallrock is sedimentary, the detrital age may reflect the sedimentary provenance of the wallrock or post-depositional cooling depending upon the thermal history. Although it is not possible to easily isolate the 1M_d polytype for direct dating of authigenic clay growth (and therefore fault growth), standard X-ray diffraction (XRD) techniques enable quantitative measurement of the abundance of each polytype in a gouge sample. Because the kinetics for the growth of large clay crystallites at low temperatures are unfavorable, the authigenic clays are typically very fine-grained (<1 μm) and generally smaller than the 2M_1 (detrital polytype) illite. Thus, high-speed centrifugation techniques can be used to create subsamples of gouge of varying size fractions and containing varying proportions of authigenic illite. If three or more grain-size fractions from a single gouge are dated, each with varying proportions of authigenic illite, the age of a sample comprising100% authigenic clay can be determined by extrapolation (see van der Pluijm et al., 2001, for details).

Our fault dating approach requires that the 1M_d polytype of illite grows during the generation of gouge and is neither inherited from the wallrock nor formed following the end of fault-slip. The observed concentration of the 1M_d polytype is concentrated in the finer-grained gouge and suggests *in situ* growth rather than inheritance, since mechanical breakdown would not preferentially affect one polytype over another. Field observations, both from the faults described below as well as in many other settings (e.g., Haines and van der Pluijm, 2008, 2010), show that fault gouge commonly preserves a crude foliation. This indicates the gouge formation under significant differential stress (i.e., is syn-tectonic). Significantly, a lack of overprinting of this fabric suggests that any post-illite-growth slip and deformation was minor. Thus, although the authigenic illite may have formed during individual slip events, during aseismic creep, or during fluid flow, the age of the 1M_d polytype provides an estimate for fault formation.

We analyzed fault gouge sampled from major thrust faults in the central Pyrenean fold-thrust belt (Fig. 1). For each sample, standard gravitational settling techniques were used to create three or four grain-size fractions, typically 2.0 to 0.4 μm, 0.4 to 0.05 μm, and <0.05 μm. The authigenic/detrital clay ratio for each subsample was estimated by modeling observed XRD patterns using WILDFIRE©, a program that calculates XRD patterns for illitic clays with a variety of crystallographic variables (Reynolds, 1993a,b). The 1σ uncertainty on the quantification of the clay components is estimated to be about 2% (Haines and van der Pluijm, 2008). Further details on gouge sample preparation and clay modeling are presented in Appendix A.

A total of 13 size fractions from four faults were dated by $^{40}Ar/^{39}Ar$ methods at the University of Michigan. To avoid the problem of argon recoil, the samples were packaged into fused silica vials and sealed prior to irradiation (van der Pluijm et al., 2001). Thus, the ^{39}Ar expelled from the crystallites during irradiation is retained for analysis (see Dong et al., 1995 for a treatment of the issue). The sample vials were broken open, the initial gas was analyzed, and the vials were then step-heated under a defocused laser until sample fusion occurred. The total gas age obtained from the vacuum-encapsulated sample is equivalent to a conventional K–Ar age.

3.2. Detrital thermochronology of syn-tectonic sediments

Although studies of river sediment loads (e.g., Milliman and Syvitski, 1992) and cosmogenic nuclides (e.g., Bierman and Steig, 1996) provide estimates of erosion rates over geologically short (<10^4 years) time periods, low-temperature thermochronology represents a key tool capable of quantifying rates of erosion over the million-year time-scales relevant to orogenesis (see Reiners and Brandon, 2006, for a recent review). Of particular relevance are approaches focused on the cooling ages preserved in detrital grains in sedimentary rocks (Bernet and Spiegel, 2004, and references therein). Many stratigraphic sections preserve continuous deposition over 10s of millions of years, enabling reconstruction of the long-term record of exhumation in a source terrane (e.g., Cerveny et al., 1988; Copeland and Harrison, 1990).

The estimation of erosion rates through detrital thermochronologic ages depends upon the lag-time, defined as the difference between the thermochronologic age and the depositional age for a sedimentary rock (Brandon and Vance, 1992; Cerveny et al., 1988). Thermochronologic ages generally represent the amount of time that has passed since a sample has cooled through a closure temperature isotherm (Dodson, 1973) at some closure depth (Z_c). Short lag-times indicate that relatively little time was needed to exhume a sample from the closure depth to the surface, implying relatively fast rates of erosion (assuming tectonic exhumation is insignificant). One challenge for relating observed lag-times to source terrane erosion rates is that rapid erosion advects both rock and heat toward the surface, altering the thermal profile of an orogen, and therefore Z_c (e.g., Brandon et al., 1998). However, it has been shown that steadily eroding mountain belts will achieve a stable thermal profile; in these situations, the system will evolve to a predictable relationship between erosion rate and lag-time (Reiners and Brandon, 2006). Numerical models can be used to infer changes in erosion rate from lag-time in non-steady-state orogens (e.g., Rahl et al., 2007).

One difficulty in detrital studies of fine-grained deposits (e.g., sandstones) comes from sedimentary mixing: individual grains in a sample may be derived from separate source areas that have different exhumation histories. Peak-fitting procedures provide a statistical basis for identifying distinct populations of grains (e.g., Brandon, 1992), but there is still uncertainty as to whether variations in the observed distribution of cooling ages reflect the evolution of a single source or are instead caused by the conflation of signal from multiple areas (Carter and Moss, 1999; Rahl et al., 2003). This ambiguity can be avoided by focusing on cobbles in a conglomerate, in which the detrital ages can clearly be related to a particular source area. For this reason, our study is focused on granitic cobbles in the Sierra de Sis body that are lithologically similar to those of the Maledeta pluton, enabling us to reconstruct the lag-time evolution of rocks derived from the Axial Zone.

Like in other mountain belts, profiles in the Pyrenees show a correlation of apatite fission-track age and elevation (Fitzgerald et al., 1999). Therefore, sediment from the modern landscape will have a range of cooling ages that reflects the ages of rocks exposed throughout the upstream drainage basin. A similar situation must have existed at times in the geologic past. This raises a potential problem for a study like ours, which seeks to track lag-time with time, because variations in the cooling age in different cobbles over time could be caused by either a) a change in erosion rate of the source region, or b) variation in the elevation in the paleo-landscape from which a sample originated. To address this issue, we developed a sampling strategy that minimizes

analytical costs while allowing us to better account for potential variability in the source terrane. For a subset of samples, we collected 40 well-rounded granitic cobbles from a given layer, took an equal sized split of each cobble, and crushed and homogenized the material. We obtained an AFT age from this aggregate sample as well as for a single cobble from each layer. The homogenized sample should include grains with ages that span the range that existed in the paleo-landscape of the pluton. This distribution provides context for the interpretation of the individual cobble samples. The apatite fission-track analysis was conducted by Paul O'Sullivan, using laser ablation inductively couple plasma mass spectrometry for U concentrations (see Donelick et al., 2005 for a description of methodology).

4. Results and interpretations

4.1. Illite age analysis

The XRD modeling of the various size fractions from gouges shows that all samples display a clear change in polytypism from relatively $2M_1$-rich (detrital polytype) in the coarse size fractions to relatively $1M_d$-rich (authigenic polytype) in the finer size fractions, supporting the implication that the $1M_d$ polytype grew at relatively low temperatures during gouge formation. A characteristic polytype quantification and associated $^{40}Ar/^{39}Ar$ degassing spectra for the same material are shown in Fig. 2. The Ar-release spectra typically do not show plateaus due to the effect of Ar recoil (see Dong et al., 1995) and because individual crystals have different ages. Therefore, the total gas age is taken as the age for each subsample (see van der Pluijm et al., 2001). Illite age analysis plots of the % detrital ($2M_1$ polytype) versus the apparent $^{40}Ar/^{39}Ar$ age of each size fraction are shown in Fig. 3. Here, we discuss new results from four Pyrenean thrusts, moving from the foreland toward the interior of the orogen (Fig. 4).

4.1.1. Boixols thrust

The Boixols thrust sensu stricto is exposed for ~32 km along strike where Jurassic to Cretaceous shelf carbonates are thrust over Late Cretaceous foredeep carbonates and shales (Ardèvol et al., 2000; Deramond et al., 1993; Simo, 1986). The fault is considered the result of inversion of an early Cretaceous extensional basin (Bond and McClay, 1995). Existing stratigraphic data (Ardèvol et al., 2000; Guillaume et al., 2008) indicate that the Boixols thrust was active during the Campanian (83–70 Ma) and became inactive at in the early Maastrichtian (70–65.5 Ma) (Deramond et al., 1993). The 71.2 ± 6.4 Ma age (Fig. 3) of authigenic illite in Boixols gouge, collected east of the town of Boixols, indicates the timing of the latest Cretaceous contractional event at this location. The fault splays to the west, and intraformational unconformities and growth strata (Mellere, 1993; Sinclair et al., 2005) and stratigraphic data (Ardèvol et al., 2000) suggest deformation there may continue into the Eocene or Oligocene.

4.1.2. Nogueres zone thrust

A southward-facing overturned thrust in the Nogueres zone is found in a kilometer-scale region of south-dipping overturned thrusts that juxtapose Paleozoic and Mesozoic units at the southern margin of the Axial Zone. The thrust has a relatively minor displacement of ~160 m (Saura, 2004), although it kinematically linked to the major Gotarta thrust (Saura and Teixell, 2006). Existing data on the timing of thrust movement are few, with motion known to predate deposition of an upper Eocene conglomerate that unconformably overlies the Nogueres thrust slice. Authigenic illite in the gouge is 56.4 ± 1.3 Ma, recording latest Paleocene to earliest Eocene activity on the Gotarta thrust.

4.1.3. Gavarnie thrust

The Gavarnie thrust marks the southern edge of the Axial zone and juxtaposes Devonian and Silurian phyllites and slates (unconformably overlain by upper Cretaceous limestones) over Triassic to late

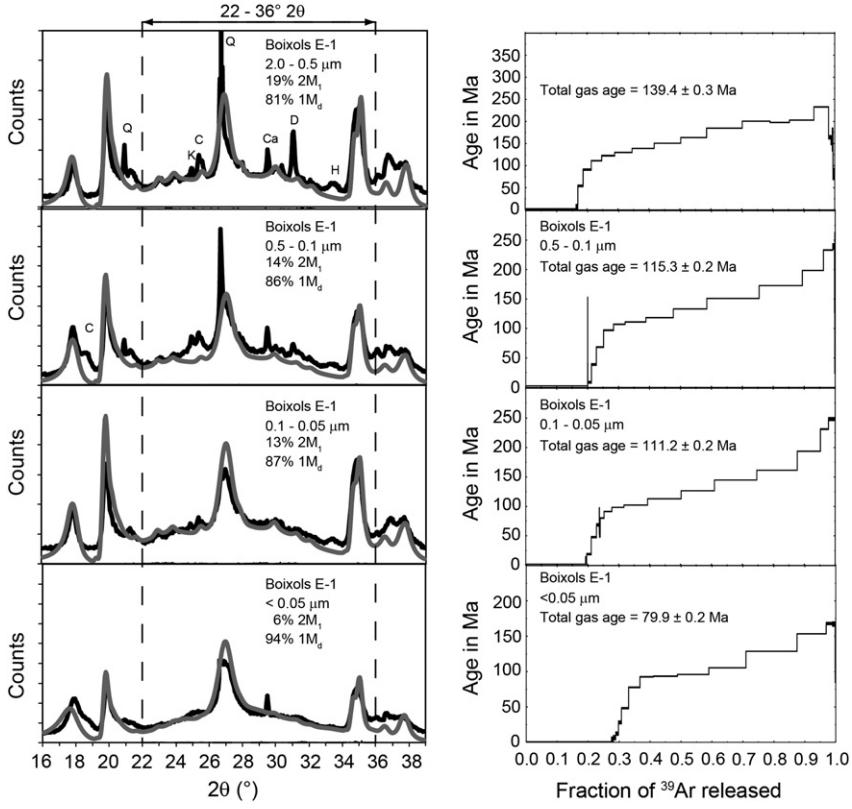

Fig. 2. Left: Representative XRD patterns (black) and modeled patterns (gray) for gouge from the Boixols thrust. Right: the corresponding $^{40}Ar/^{39}Ar$ spectra for the same samples.

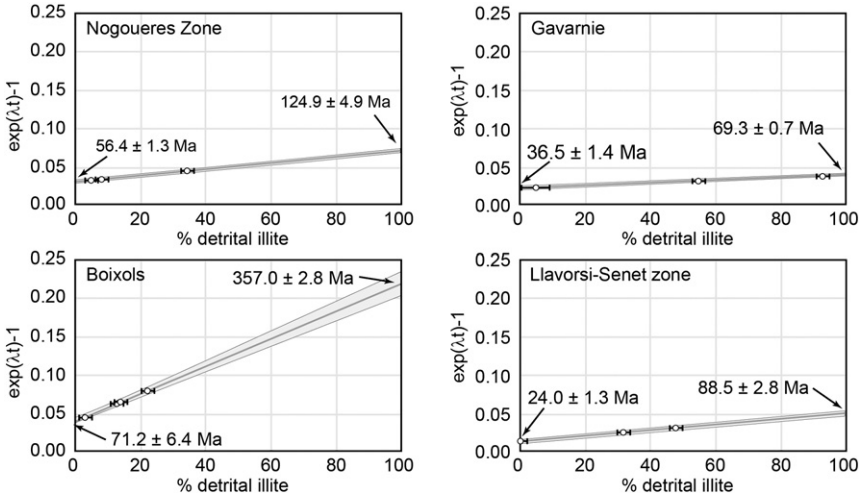

Fig. 3. Illite age analysis plots, showing percentage detrital components and ages of three fractions of four fault gouge samples. Function $e^{(\lambda t-1)}$ is related to detrital illite, where λ is decay constant and t is time.

Cretaceous redbeds and limestones (van Lith, 1965). The outcrop sampled is 200 m north of the hangingwall cutoff for the Gavarnie nappe where Cretaceous limestones unconformably overlie Devonian phyllites. To the southeast along strike, the fault is observed to cut Cuesian (52–48 Ma) turbidites but not latest Eocene and Oligocene sediments (Labaume et al., 1983), thus bracketing fault activity from earliest to latest Eocene. The age of authigenic illite in the sheared phyllite of 36.5 ± 1.4 Ma reveals the youngest record of fault movement on the Gavarnie thrust is the latest Eocene. The very small amount of material obtained for the <0.05 μm size fraction resulted in an atypically lower-quality XRD pattern for polytype modeling, so a 1σ estimate of 5% was used for this size fraction in the error analysis.

The Gavarnie thrust has a complex history of fluid flow (Banks et al., 1991; Grant et al., 1990; McCaig et al., 1995; McCaig et al., 2000), with migration of at least two pulses of 250–300 °C saline brines derived from underlying Triassic redbeds and Silurian phyllites observed in Gavarnie mylonites. These infiltration events represent a potential cause of authigenic illite growth other than fault activity. However, we interpret our authigenic illite age to record slip on the Gavarnie fault for two reasons: 1) overprinting relations in the field indicate that brittle deformation postdates earlier mylonitization, so gouge formation occurred after fluid-flow; 2) the estimated fluid temperatures are high enough that it would grow illite primarily as the $2M_1$ polytype rather than the low-temperature $1M_d$ polytype that grows at temperatures <200 °C (Srodon and Eberl, 1984). Therefore, we interpret the $1M_d$ illite as cogenetic with the lower-temperature deformation also recorded by cohesive fault breccias, dating the last major event on this fault.

The age of the detrital component (69.3 +/− 0.7 Ma) of the Gavarnie thrust is interpreted as the time of early, high-temperature deformation and mylonitization along the Gavarnie thrust. In outcrop, structurally early carbonate mylonites are overprinted by more brittle breccias and clay gouges, indicating a transition from crystal-plastic to elasto-frictional processes during progressive deformation. The hangingwall cutoff of the late Cretaceous unconformity is spectacularly exposed at the Plan de Llari outcrop 200 m down-dip, and thus indicates the burial depth of the phyllites in the immediate hangingwall to be <0.2 km during the Cenomanian (100–94 Ma). The thickness of the Cretaceous and Paleogene sections overlying the late Cretaceous unconformity at Plan de Llari is ~2.5 km, and so at 69 Ma when the $2M_1$ component of the gouges began trapping significant daughter product, the immediate hangingwall of the thrust had been buried no more than 3 km. For measured diffusion parameters of Ar in muscovite ($D_o = 4\ cm^2/s$; $E = 64$ kcal/mol) (Harrison et al., 2009) and grain sizes appropriate for illite (effective diffusion radius = 0.1 to 1.0 μm), cooling rates of 1 to 10 °C/Ma predict effective closure temperatures in the range of 250 to 310 °C (calculation made using the software Closure by Brandon, described

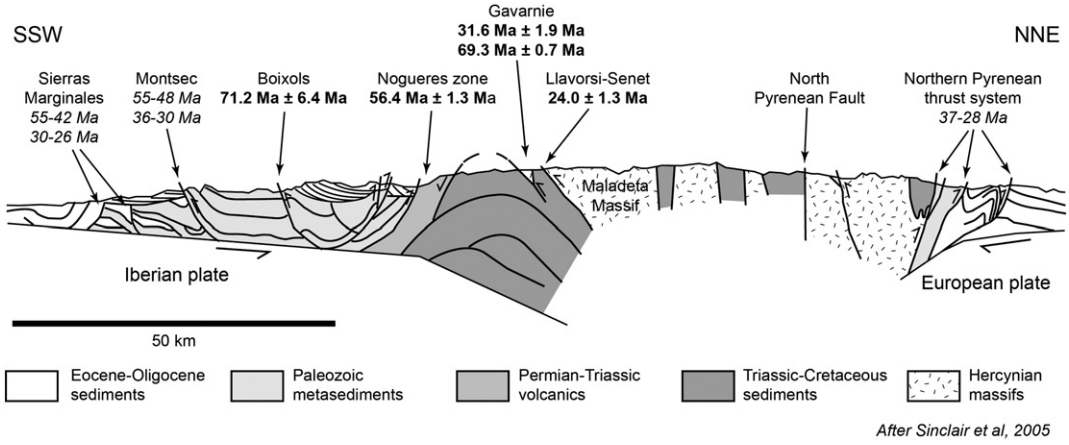

Fig. 4. A cross-section through the central Pyrenees (after Sinclair, 2008), with ages of fault activity from this (bold) and previous (italics) studies. See text for details.

in Ehlers et al., 2005). Thus, even for very high geothermal gradients, the observation of carbonate mylonites in the fault zone and young $^{40}Ar/^{39}Ar$ ages in detrital micas in the gouge forming at depths <3 km requires that the temperatures of 200–300 °C indicated by both the carbonate mylonite fault rocks and the $^{40}Ar/^{39}Ar$ ages of the detrital micas (the $2M_1$ component) record the passage of the 250–300 °C basinal fluids documented by McCaig et al. (1995, 2000). As the evidence for hydrothermal alteration is confined to the fault zone, we conclude that the ages of both the detrital and authigenic components at Gavarnie date faulting events, an early mylonization event aided by high-temperature fluids migrating up the detachment at 70 Ma, and a late event indicated by the growth of the low-temperature polytype of illite in gouge at 35 Ma. Our result supports the inference of Metcalf et al. (2009), who used K-spar multi-diffusion domain modeling from footwall samples to argue that slip on the Gavarnie fault began at about 70 Ma.

4.1.4. Llavorsi-Senet zone thrust

The thrust in the Llavorsi-Senet thrust zone is the most inboard sampled thrust and juxtaposes Cambro-Ordovician metapelites of the Orri and Erta thrust sheets. The age of the thrust has been uncertain, as it juxtaposes Paleozoic rocks over its entire length. Section-balancing implies it is younger than the Nogueres thrusts, which have been tilted southward post-slip (Muñoz, 1992). The age of the authigenic illite in the gouge is 24.0 ± 1.3 Ma, refining an inferred early Oligocene age based on the syn-tectonic Senterada conglomerates that unconformably overlie strongly tilted Nogueres Zone structures and contain clasts derived from the hangingwall Orri thrust sheet (Saura and Teixell, 2000).

4.1.5. The thermal history of the host rock

In addition to providing the age of the authigenic clays formed during faulting, the illite age analysis technique also estimates the age of the $2M_1$ illite in gouge. Van der Pluijm et al. (2001) proposed that this age represents the mean age of cooling of the source area through the illite closure temperature, and therefore reflected sedimentary provenance of the wallrock. In the Pyrenees, the $2M_1$ ages for the studied faults young toward the core of the mountain belt, from 357 ± 2.8 Ma for the Boixols to 69.3 Ma 0.7 ± for Gavarnie. The Boixols age clearly predates Pyrenean orogenesis and we interpret it to reflect provenance as suggested by van der Pluijm et al. (2001). However, the more inboard samples show Cretaceous ages that post-date the Paleozoic and Mesozoic depositional ages of juxtaposed units. We note that maximum metamorphic temperatures typically increase toward the interior of orogenic wedges (e.g., Barr et al., 1991). Therefore, we propose that the host-rock ages of the more inboard samples reflect at least partial resetting of the $2M_1$ illite during Pyrenean metamorphism. Metcalf et al. (2009) use K-spar ^{40}Ar–^{39}Ar multi-diffusion domain modeling to demonstrate peak temperatures in the Axial Zone reaching 270 to 280 °C, which is similar to the effective closure temperature for very fine illite (see above). More generally, we propose that in settings where bedrock has been heated about >280 °C, the $2M_1$ illite will reflect exhumation-related cooling (e.g., Haines and van der Pluijm, 2008).

4.2. Detrital thermochronology

We present thermochrologic results from eight cobble samples derived from throughout the Paleogene Sierra de Sis conglomerate body. Depositional ages are estimated from rare biostratigraphic data, correlation with better understood strata from the adjacent Graus-Tremp Basin (Vincent, 2001), and limited magnetostratigraphy (Beamud et al., 2003; Beamud et al., 2010). Samples were collected from several units in the conglomerate body, including the Cornudella, Sis, and Collegats Formations. The stratigraphic ages shown in Fig. 5 are based on the stratigraphic column from Vincent (2001) with revisions to the lower part of the section based on more recent magnetostratigraphy (Beamud et al., 2010). The sampled horizons span from about 41 to 30 Ma.

The central ages for the apatite fission-track analyses range from 43.0 to 57.2 Ma (Table 1; Fig. 5). Four of the eight samples fail a χ^2 test (Galbraith, 1981), suggesting that the apatites for these cobbles do not belong to a single age population; a similar result was reported by Beamud et al. (2010). For these four samples, the additional variation in the single grain ages likely reflects variable annealing caused by chemical differences between the apatites (O'Sullivan and Parrish, 1995; Tagami and O'Sullivan, 2005). Binomial peak-fitting (Galbraith and Green, 1990) was applied to all samples to identify multiple age components, using the software RadialPlotter (Vermeesch, 2009). The results of the peak-fitting are shown in Fig. 6.

As noted above (Section 3.2), we have analyzed both single cobbles and an aggregate sample from three horizons (Fig. 7). The spread of grain ages is greater for the aggregate sample, consistent with it being a mixture of grains from sources with variable histories. The AFT ages from the individual cobbles generally are similar to those of the corresponding aggregate sample, indicating that the cobble samples are representative of the landscape exposed at the time of exhumation. In the case of sample C49, the central age is ~9 Ma older than both the aggregate sample and a second cobble collected from the same horizon (Fig. 5). When compared to the aggregate sample, C49 lacks a population of young grains (Fig. 7), suggesting this sample cooled early and was derived from high in the paleo-landscape. This interpretation is supported by the modeled time–temperature history (discussed below) for this sample, which shows an early and relatively slow cooling (Fig. 6).

The observed detrital cooling ages cluster around 45 Ma and do not show a clear trend over time (Fig. 5A). Also plotted are recent AFT results on granitic cobbles from the Sis and the nearby deposits in La

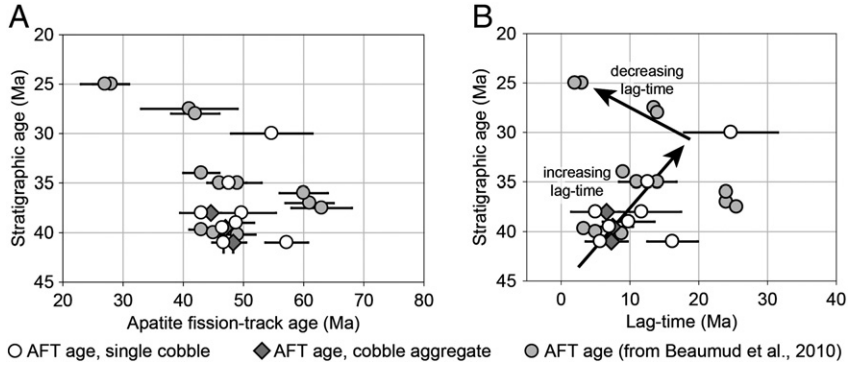

Fig. 5. A) Depositional age versus apatite fission-track age for individual cobbles (white circles) and aggregate samples (dark gray diamonds). The gray circles are taken from grantitic cobbles in the Sis, La Pobla, and Senterada basins, as reported by (Beamud et al., 2010). B) Depositional age versus apatite fission-track lag-time. Lag-times decrease moving upsection, indicating a decrease in erosion rate with time.

Table 1
Apatite fission-track data.

Sample	Latitude (°N)	Longitude (°E)	Elevation (m)	Depositional age (Ma)	Stratigraphic unit	Number of grains	Dpar (μm)	Apatite fission-track central age ± 1σ (Ma)	Number of confined tracks	Mean track length (μm)	χ^2 probability (%)
060709-2	42.36	0.68	1543	30.0 ± 3.0	Collegats Formation	23	2.11	47.6 ± 2.9	129	14.21 ± 1.34	11.66
060711-3	42.327	0.623	1627	35.0 ± 1.0	Sis 3 member	25	1.64	54.7 ± 6.8	107	13.75 ± 1.29	0.02
Sis 2a	42.323	0.620	1504	38.0 ± 0.5	Sis 2 member	40	1.68	49.7 ± 5.7	151	13.28 ± 1.67	66.29
Sis 2 aggregate	42.323	0.620	1504	38.0 ± 0.5	Sis 2 member	119	1.75	44.6 ± 1.7	–	–	–
060711-7	42.322	0.620	1504	38.0 ± 0.5	Sis 2 member	24	1.59	43.0 ± 3.5	120	13.90 ± 1.18	0.01
060713-5	42.316	0.618	1397	39.0 ± 1.5	Sis 1 member	25	1.59	48.8 ± 3.0	120	14.23 ± 1.38	16.22
Sis 1.1	42.312	0.617	1278	39.5 ± 1.5	Sis 1 member	39	1.77	46.5 ± 2.4	205	13.56 ± 1.46	0.00
Sis 1.1 aggregate	42.312	0.617	1278	39.5 ± 1.5	Sis 1 member	116	1.74	47.0 ± 1.9	–	–	–
060710-3	42.290	0.614	1193	41.0 ± 1.0	Cornudella Formation	24	1.63	46.7 ± 1.9	109	13.37 ± 1.24	5.92
C 49	42.290	0.614	1197	41.0 ± 1.0	Cornudella Formation	40	2.08	57.2 ± 3.5	203	14.20 ± 1.59	0.16
C49 aggregate	42.290	0.614	1197	41.0 ± 1.0	Cornudella Formation	118	1.85	48.3 ± 2.1	–	–	–

Pobla and Senterada (Beamud et al., 2010), which show a similar pattern. The generally uniform ages result in an increasing lag-time upsection (Fig. 5B), from about 5 Ma to >15 Ma in over 10 million - years of deposition, implying a decrease in erosion rate in the Middle to Late Eocene (e.g., Rahl et al., 2007). Beamud et al. (2010) do observe several old (~62 Ma) apatite fission-track ages that give large lag-times in Middle Eocene sediments, but given the similarity in the ages to our sample C49, we interpret these samples to have derived from high in the paleo-landscape and insensitive to the rapid Middle Eocene exhumation. Oligocene sediments have young ages with short lag-times, indicating a rapid transition back to rapid erosion in the Early Oligocene (Beamud et al., 2010).

To further explore the thermal history of the source region, we have modeled apatite track-length distributions using the HeFTy software package (Ketcham, 2005). Our average track-length measurement for the Durango apatite standard 1.55 μm is less than the 1.91 μm value from Carlson et al. (1999) for the same etching conditions (5.5 M HNO_3 for 20 s) that is incorporated into Ketcham et al. (2007) built into HeFTy. Therefore, we scaled our track-length measurements for model input.

Several time–temperature constraints were incorporated into the HeFTy models. First, each time–temperature path begins at a temperature in excess of 160 °C prior to 80 Ma, reflecting the pre-annealing history of each grain. The time of deposition provides a second constraint, with an assumed surface temperature of 15 ± 5 °C. Third, given post-depositional burial, the model explores the time–temperature space between 10 and 120 °C prior to 20 Ma. Within these constraints, HeFTy generates random time–temperature paths and compares the predicted and observed track-length observations. The quality of fit for each model is assessed using either the Kuiper's or Kolmogorov–Smirnov statistic (Ketcham, 2005). Models were randomly generated until 100 time–temperatures paths yielding "good" fits with the data were identified.

The track-length modeling results (Fig. 6) indicate that most samples preserve a period of rapid cooling generally around 45 Ma. Several samples, particularly lower the stratigraphic section, may have experienced reheating during burial to temperatures that approached 80 °C. These samples could be partially reset and experienced some age reduction (see Beamud et al., 2010). However, the track-length measurements are generally long (>13.5 μm), suggesting that post-deposition age reduction is minimal.

5. Discussion and conclusions

The record of brittle deformation in the central Pyrenees fold-thrust belt is summarized in Figs. 4 and 8. Previous structural and paleomagnetic work has demonstrated that fault activity in the area occurred during distinct deformational pulses (e.g., Meigs, 1997; Meigs and Burbank, 1997). The fault-gouge ages reported here complement and significantly refine this record, and show that out-of-sequence thrusting was an important process in the development of the wedge. Our new data indicate motion on the Boixols thrust at ~72 Ma, and the formation of the early hydrothermally-aided carbonate mylonites on the Gavarnie thrust at ~69 Ma, confirming the onset of Pyrenean convergence and associated thrust deformation by the late Cretaceous. This early pulse of deformation is followed by a period of apparent tectonic quiescence, characterized by low convergence rates and deformation accommodated primarily on inverted Cretaceous extensional faults (Vergés et al., 2002). By the late Paleocene–early Eocene, however, active thrust deformation resumes and is observed throughout the Pyrenean wedge. Thrusting occurred on the Sierres Marginales and Montsec thrusts in the frontal part of the wedge (Meigs, 1997), with coeval deformation observed inboard in the Nogueres zone (~56 Ma fault gouge) and on the Gavarnie thrust (Labaume et al., 1985), as well as in the North Pyrenean fold-thrust belt (Fischer, 1984).

During most of the Eocene (51 and 36 Ma), there is little evidence for within-wedge deformation, and Meigs and Burbank (1997) infer this was a period characterized by stable sliding of the wedge on its base. Thrust activity resumes between 36 and 28 Ma, with shortening at the leading edge of the thrust belt (Meigs and Burbank, 1997) as well as along the Gavarnie fault (with a gouge age of ~32 Ma). A final period of early Oligocene faulting in the central portion of the Axial Zone is recorded by the ~24 Ma gouge age on the Llavorsi-Senet thrust.

Similar to the history of within-wedge brittle deformation, the record of erosion in the Axial Zone is also characterized by discrete episodes. The thermal models of apatite fission-track data from cobbles in syn-tectonic conglomerates record rapid exhumation from ~50 to 42 Ma. The onset of rapid erosion (>0.25 mm/a) at ~50 Ma has also been recognized from bedrock thermochronology with higher closure temperature systems, including zircon fission-track (Sinclair et al., 2005) and K-feldspar ^{40}Ar–^{39}Ar (Metcalf et al., 2009). This pulse of exhumation was followed by a period of slower erosion, indicated by the increasing apatite fission-track lag-time observed in sediments

Fig. 6. Left: Radial plots of single grain apatite fission-track ages. The component age and proportion of grains in each subpopulation are indicated for samples that fail the χ^2 test. Right: Time–temperature models based on inversion of track-length distributions using the HeFTy software package. Model constraints are indicated by the black boxes. Envelopes of good (light gray) and excellent (dark gray) paths are shown. The "good" solution envelope is defined by 100 randomly generated paths. The models are consistent with rapid cooling between 50 and 40 Ma.

060709-2
Strat. Age ~ 30 Ma
AFT Age: 47 ± 3 Ma

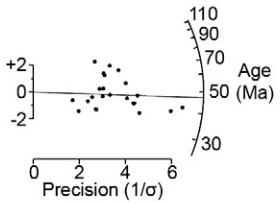

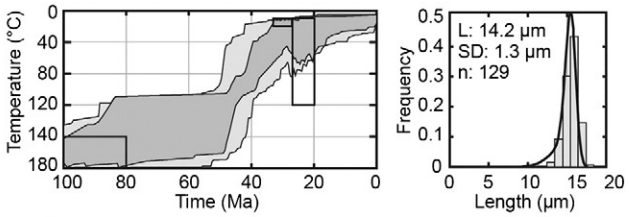

060711-3
Strat. Age ~ 35 Ma
AFT Age: 55 ± 7 Ma

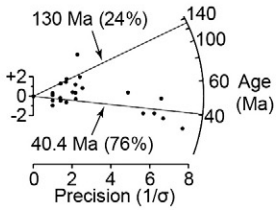

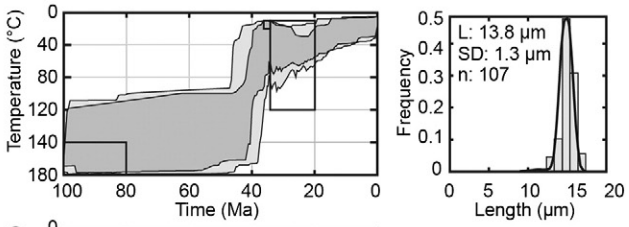

Sis 2a
Strat. Age ~ 38 Ma
AFT Age: 50 ± 6 Ma

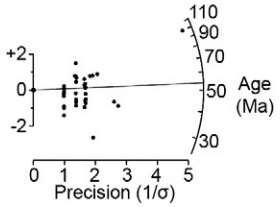

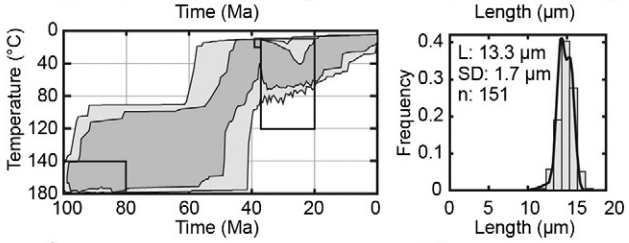

060711-7
Strat. Age ~ 38 Ma
AFT Age: 43 ± 4 Ma

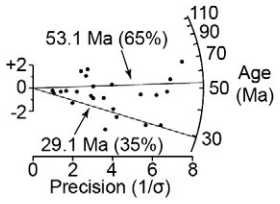

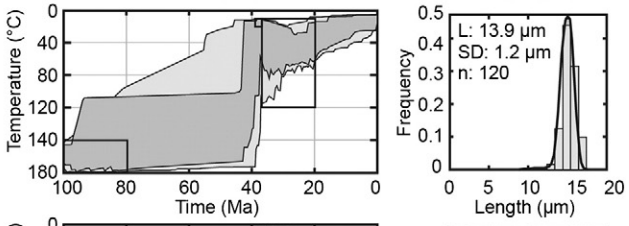

060713-5
Strat. Age ~ 39 Ma
AFT Age: 49 ± 3 Ma

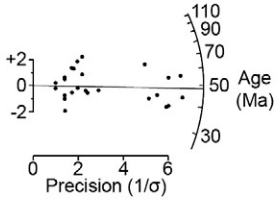

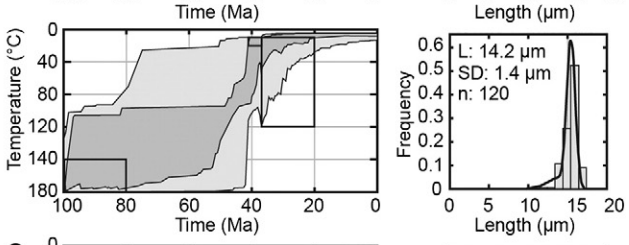

Sis 1-1a
Strat. Age ~ 39.5 Ma
AFT Age: 47 ± 2 Ma

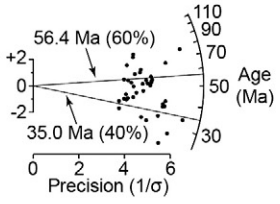

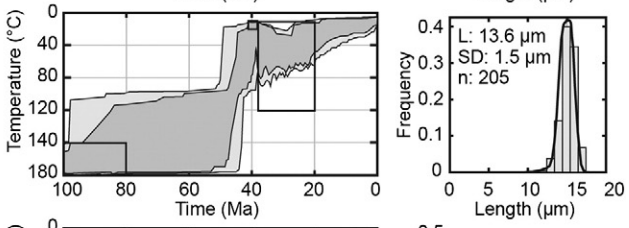

060710-3
Strat. Age ~ 41 Ma
AFT Age: 47 ± 2 Ma

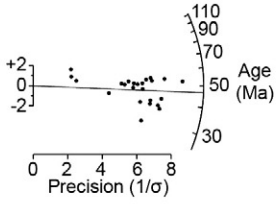

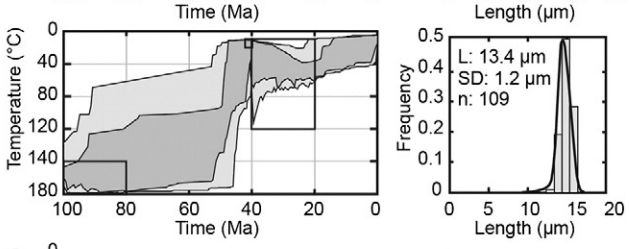

C49
Strat. Age ~ 41 Ma
AFT Age: 48 ± 2 Ma

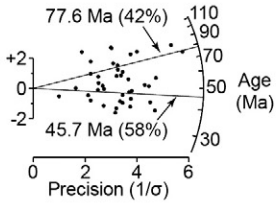

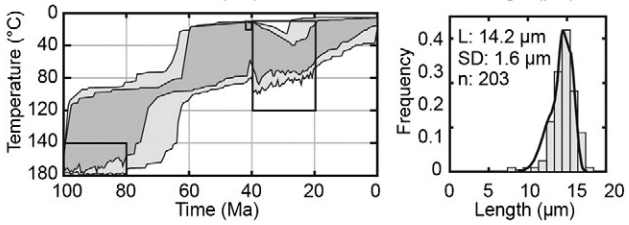

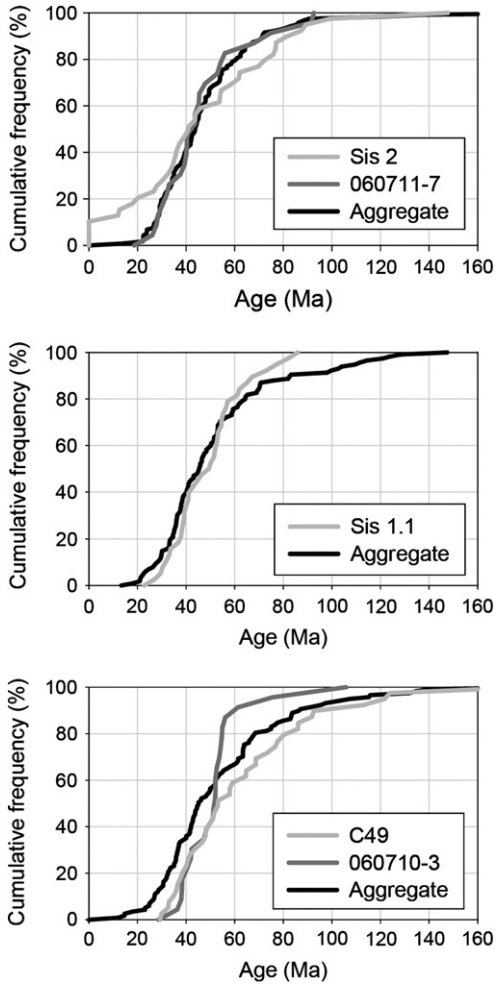

Fig. 7. Cumulative frequency diagram showing age distributions for individual cobble and aggregate cobble distributions from three horizons (see text for details).

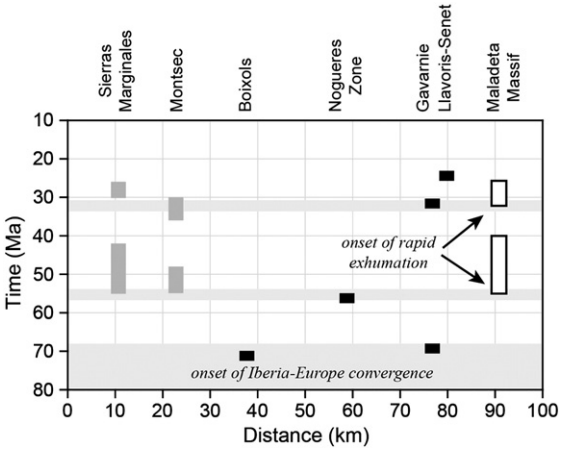

Fig. 8. Summary diagram showing the record of fault-slip and Axial Zone exhumation in the central Pyrenees. Gray boxes correspond to periods of fault motion inferred in previous studies (Burbank et al., 1992b; Meigs et al., 1996; Meigs and Burbank, 1997). Black boxes represent illite-age analysis of fault gouge (this study). The white boxes represent periods of rapid exhumation (>0.25 mm/a) inferred from this and previous studies (Beamud et al., 2010; Fitzgerald et al., 1999; Metcalf et al., 2009; Sinclair et al., 2005).

deposited between 41 and 30 Ma. Around 32 Ma, age-elevation profiles and thermal modeling showed that rapid exhumation resumed in the Axial Zone (Fitzgerald et al., 1999; Metcalf et al., 2009; Sinclair et al., 2005). This coincides with activation of the Gavarnie Fault in the wedge-interior, marking a period of underplating-induced growth of the Pyrenean antiformal stack, with the most rapidly eroding region consequently migrating south of the Axial Zone (Sinclair et al., 2005).

The detailed records of thrust faulting and exhumation in the Maledeta pluton in the Axial Zone reveal a temporal correlation between thrust faulting and erosion (Fig. 8). Deformation in the Pyrenean wedge occurred during discrete episodes, from ~56 to 48 Ma and later around ~36 to 30 Ma. Prior to each of these deformational pulses, exhumation in the Axial Zone was slow. However, following the initiation of the thrust episodes, erosion accelerated, with rapid Middle Eocene cooling preserved in the syn-tectonic cobbles of the Sis Conglomerate body and Early Oligocene exhumation documented in the Axial Zone bedrock.

The new data presented here document a complex pattern of deformation within the Pyrenean wedge. Unlike simple physical and numerical models that predict forward-stepping development of thrust activity (e.g., Davis et al., 1983), our observations indicate that deformation occurred throughout the wedge during its evolution. During certain intervals, such as the early Eocene or early Oligocene, active deformation occurred simultaneously on structures in both the front and interior of the wedge. A similar result has been found in the Canadian Rockies (van der Pluijm et al., 2006), where faults from throughout the fold-thrust belt were found to be active in one of two main deformational pulses. These conclusions support the idea that tectonism within orogenic belts is generally not steady, but instead may exhibit significant changes in the rates of deformation and exhumation over time.

Supplementary materials related to this article can be found online at doi:10.1016/j.epsl.2011.04.036.

Acknowledgments

Rahl was supported by a Turner Post-doctoral Research Fellowship from the Department of Geological Sciences, University of Michigan. Research was supported by the National Science Foundation, grants EAR-0629331 and EAR-0738435. This manuscript benefitted from constructive comments from Hugh Sinclair, an anonymous reviewer, and editor T. Mark Harrison. We thank Todd Ehlers for key discussions on detrital thermochronology. We thank Paul O'Sullivan of Apatite to Zircon, Inc., for performing the apatite fission-track analyses.

References

Ardèvol, L., Klimowitz, J., Malagón, J., Nagteggal, P., 2000. Depositional sequence response to foreland deformation in the Upper Cretaceous of the Southern Pyrenees, Spain. AAPG Bulletin 84, 566–587.
Armstrong, F., Oriel, S., 1965. Tectonic development of Idaho-Wyoming thrust belt. AAPG Bulletin 49, 1847–1866.
Banks, D., Davies, G., Yardley, B., McCaig, A., Grant, N., 1991. The chemistry of brines from an alpine thrust system in the central Pyrenees: an application of fluid inclusion analysis to the study of fluid behavior in orogenesis. Geochimica et Cosmochimica Acta 55, 1021–1030.
Barr, T.D., Dahlen, F.A., McPhail, D.C., 1991. Brittle frictional mountain building 3. Low-grade metamorphism. J. Geophysical Res. 96, 10319–10338.
Beamud, E., Garcés, M., Cabrera, L., Muñoz, J.A., Almar, Y., 2003. A new middle to late Eocene continental chronostratigraphy from NE Spain. Earth Planetary Sci. Lett. 216, 501–514.
Beamud, E., Muñoz, J.A., Fitzgerald, P.G., Baldwin, S.L., Garcés, M., Cabrera, L., Metcalf, J.R., 2010. Magnetostratigraphy and detrital apatite fission track thermochronology in syntectonic conglomerates: constraints on the exhumation of the South-Central Pyrenees. Basin Research, 23, 309–331.
Beaumont, C., Fullsack, P., Hamilton, J., 1992. Erosional control of active compressional orogens. In: McClay, K.R. (Ed.), Thrust Tectonics. Chapman & Hall, London, United Kingdom, pp. 1–18.
Beaumont, C., Muñoz, J.A., Hamilton, J., Fullsack, P., 2000. Factors controlling the Alpine evolution of the central Pyrenees inferred from a comparison of observations and geodynamical models. J. Geophysical Res. B Solid Earth Planets 105, 8121–8145.
Bernet, M., Spiegel, C., 2004. Introduction: detrital thermochronology. In: Bernet, M., Spiegel, C. (Eds.), Detrital Thermochronology; Provenance Analysis, Exhumation, and Landscape Evolution of Mountain Belts., Geological Society of America (GSA). Boulder, CO, United States. 2004, pp. 1–6.

Bierman, P., Steig, E.J., 1996. Estimating rates of denudation using cosmogenic isotope abundances in sediment. Earth Surface Processes Landforms 21, 125–139.
Bond, R., McClay, K., 1995. Inversion of a Lower Cretaceous extensional basin, south-central Pyrenees, Spain. In: Buchanan, J., Buchanan, P. (Eds.), Basin Inversion, volume 88. Geological Society of London Special Publications, pp. 415–431.
Brandon, M.T., Roden-Tice, M.K., Garver, J.I., 1998. Late Cenozoic exhumation of the Cascadia accretionary wedge in the Olympic Mountains, Northwest Washington State. Geological Soc. Am. Bull. 110, 985–1009.
Brandon, M.T., 1992. Decomposition of fission-track grain-age distributions. Am. J. Sci. 292, 535–564.
Brandon, M.T., Vance, J.A., 1992. Zircon fission-track ages for the Olympic subduction complex and adjacent Eocene basins, western Washington State: Washington Division of Geology and Earth Resources, pp. 92–96. Open File Report.
Burbank, D.W., Puigdefàbregas, C., Muñoz, J.A., 1992a. The chronology of Eocene tectonics and stratigraphic development of the eastern Pyrenean foreland basin, northeast Spain. Geological Soc. Am. Bull. 104, 1101–1120.
Burbank, D.W., Vergés, J., Muñoz, J.A., Bentham, P., 1992b. Coeval hindward- and foreward-imbricating thrusting in the south-central Pyrenees, Spain: timing and rates of shortening and deposition. Geological Soc. Am. Bull. 104, 3–17.
Carlson, W.D., Donelick, R.A., Ketcham, R.A., 1999. Variability of apatite fission-track annealing kinetics; I. Exp. results Am. Mineralogist 84, 1213–1223.
Carter, A., Moss, S.J., 1999. Combined detrital-zircon fission-track and U–Pb dating: a new approach to understanding hinterland evolution. Geology 27, 235–238.
Cerveny, P.F., Naeser, N.D., Zeitler, P.K., Naeser, C.W., Johnson, M.N., 1988. History of uplift and relief of the Himalaya during the past 18 million years: evidence from fission-track ages of detrital zircons from sandstones of the Siwalik Group. In: Kleinspehn, K., Paola, C. (Eds.), New Perspectives in Basin Analysis. Springer-Verlag, New York, pp. 43–61.
Choukroune, P., Daignières, M., Deramond, J., Grasso, J.R., Hirn, A., Marthelot., J.N, Mattauer, M., Seguret, M., Damotte, B., Roure, F., Cazes, M., Toreilles, G., Villien, A., Mediavila, F., Vauthier, A., Banda, E., Fontbote, J.M., Gallart, J., Santanach, P., Surinach, E., Barnolas, A., Del Valle, J., Plata, J.L., Berastagui, X., Muñoz, J.A., Puigdefabregas, C., Rivero, A., Arrieta, A., Camara, P., Garrido, A., Martinez, J., et al., 1989. The ECORS Pyrenean deep seismic profile reflection data and the overall structure of an orogenic belt. Tectonics 8, 23–39.
Coney, P.J., Munoz, J.A., McClay, K., Evenchick, C.A., 1996. Syn-tectonic burial and post-tectonic exhumation of an active foreland thrust belt, southern Pyrenees, Spain. J. Geological Soc. London 153, 9–16.
Copeland, P., Harrison, T.M., 1990. Episodic rapid uplift in the Himalaya revealed by (super 40) Ar/ (super 39) Ar analysis of detrital K-feldspar and muscovite. Bengal Fan Geology Boulder 18, 354–357.
Dahlen, F.A., Suppe, J., 1988. Mechanics, growth, and erosion of mountain belts. In: Clark Sydney Jr., P., Burchfiel, B.C., Suppe, J. (Eds.), Processes in Continental Lithospheric Deformation. : Geological Society of America (GSA), volume 218. Special Paper — Geological Society of America, Boulder, CO, United States, pp. 161–178.
Davis, D., Suppe, J., Dahlen, F.A., 1983. Mechanics of fold-and-thrust belts and accretionary wedges. J. Geophysical Res. 88, 1153–1172.
Deramond, J., Souquet, P., Wallez, M.J.F., Specht, M., 1993. Relationships between thrust tectonics and sequence stratigraphy by surfaces in foredeeps: models and examples from the Pyrenees. In: Williams, G.D., Dobb, A. (Eds.), Tectonics and Seismic Sequence Stratigraphy, volume 71. Geological Society of London Special Publication, London, pp. 193–219.
Dodson, M.H., 1973. Closure temperature in cooling geochronological and petrological systems. Contrib. Mineralogy Petrology 40, 259–274.
Donelick, R.A., O'Sullivan, P.B., Ketcham, R.A., 2005. Apatite fission-track analysis. Rev. Mineralogy Geochem. 58, 49–94.
Dong, H., Hall, C.M., Peacor, D.R., Halliday, A.N., 1995. Mechanisms of argon retention in clays revealed by laser 40Ar – 39Ar dating. Science 267, 355–359.
Ehlers, T.A., Chaudhri, T., Kumar, S., Fuller, C.W., Willett, S.D., Ketcham, R.A., Brandon, M.T., Belton, D.X., Kohn, B.P., Gleadow, A.J.W., Dunai, T.J., Fu, F.Q., 2005. Computational tools for low-temperature thermochronometer interpretation. Rev. Mineralogy Geochem. 58, 589–622.
Evans, N.G., Gleizes, G., LeBlanc, D., Bouchez, J.L., 1998. Syntectonic emplacement of the Maladeta granite (Pyrenees) deduced from relationships between Hercynian deformation and contact metamorphism. J. Geological Soc. London 155, 209–216.
Farrell, S., Williams, G., Atkinson, C., 1985. Constrains on the age of movement of the Montsec and Cotiella thrusts, south central Pyrenees, Spain. J. Geological Soc. 144, 907–914.
Fischer, M.W., 1984. Thrust tectonics in the North Pyrenees. J. Struct. Geology 6, 721–726.
Fitzgerald, P.G., Munoz, J.A., Coney, P.J., Baldwin, S.L., 1999. Asymmetric exhumation across the Pyrenean orogen: implications for the tectonic evolution of a collisional orogen. Earth Planetary Sci. Lett. 173, 157–170.
Galbraith, R.F., 1981. On statistical models for fission-track counts. J. Mathematical Geology 13, 471–478.
Galbraith, R.F., Green, P.F., 1990. Estimating the component ages in a finite mixture. Nuclear Tracks Radiation Measurements 17, 197–206.
Gibson, M., Sinclair, H.D., Lynn, G., Stuart, F., 2007. Late-to-post-orogenic exhumation of the Central Pyrenees revealed through combined thermochronological data and modeling. Basin Res. 19, 323–334.
Grant, N., Banks, D., McCaig, A., Yardley, B., 1990. Chemistry, source and behavior of fluids in Alpine thrusting of the Central Pyreneees. J. Geophysical Res. 95, 9123–9131.
Grathoff, G.H., Moore, D.M., Hay, R.L., Wemmer, K., 2001. Origin of illite in the lower Paleozoic of the Illinois basin: evidence for brine migrations. Geology Soc. Am. Bull. 113, 1092–1104.
Guillaume, B., Dhont, D., Brusset, S., 2008. Three-dimensional geologic imaging and tectonic control on stratigraphic architecture: Upper Cretaceous of the Trem Basin (south-central Pyrenees, Spain). AAPG Bulletin 92, 249–269.
Haines, S.H., van der Pluijm, B.A., 2008. Clay quantification and Ar – Ar dating of synthetic and natural gouge: application to the Miocene Sierra Mazatán detachment fault, Sonora, Mexico. J. Struct. Geology 30.
Haines, S.H., van der Pluijm, B.A., 2010. Dating the detachment fault system of the Ruby Mountains, Nevada: significance for the kinematics of low-angle normal faults. Tectonics 29.
Harrison, T.M., Célérier, J., Aikman, A.B., Hermann, J., Heizler, M.T., 2009. Diffusion of 40Ar in muscovite. Geochimica Cosmochimica Acta 73, 1039–1051.
Ketcham, R.A., 2005. Forward and inverse modeling of low-temperature thermochronometry data. Rev. Mineralogy Geochemistry 58, 275–314.
Ketcham, R.A., Carter, A., Donelick, R.A., Barbarand, J., Hurford, A.J., 2007. Improved measurement of fission-track annealing in apatite using c-axis projection. Am. Mineralogist 92, 789–798.
Konstantinovskaia, E., Malavieille, J., 2005. Erosion and exhumation in accretionary orogens: experimental and geological approaches. Geochem. Geophys. Geosyst. 6.
Koons, P.O., 1990. Two-sided orogen; collision and erosion from the sandbox to the Southern Alps. NZ Geology Boulder 18, 679–682.
Labaume, P., Mutti, E., Séguret, M., Rosell, J., 1983. Mègaturbidtites carbonates du basin turbiditique de L'Eocène inférieur et moyen sud-pyrénéen. Bull. Geol. Soc. Fr. 7, 927–941.
Labaume, P., Séguret, M., Seyve, C., 1985. Evolution of a turbiditic foreland basin and analogy with an accretionary prism: example of the Eocene south-central Pyrenean basin. Tectonics 4, 661–685.
Ledo, J., Conxi, A., Pous, J., Queralt, P., Marcuello, A., Muñoz, J.A., 2000. New geophysical constraints on the deep structure of the Pyrenees. Geophysical Res. Lett. 27, 1037–1040.
McCaig, A., Wayne, D., Marshall, J., Banks, D., Henderson, I., 1995. Isotopic and fluid inclusion studies of fluid movement along the Gavarnie Thrust, central Pyrenees: reaction fronts in carbonate mylonites. Am. J. Sci. 295, 309–343.
McCaig, A., Wayne, D., Rosenblum, J., 2000. Fluid expulsion and dilatancy plumbing during thrusting in the Pyrenees: Pb and Sr isotopic evidence. Geological Soc. Am. Bull. 112, 1199–1208.
Meigs, A.J., 1997. Sequential development of selected Pyrenean thrust faults. J. Struct. Geology 19, 481–502.
Meigs, A.J., Burbank, D.W., 1997. Growth of the South Pyrenean orogenic wedge. Tectonics 16, 239–258.
Meigs, A.J., Vergés, J., Burbank, D.W., 1996. Ten-million-year history of a thrust sheet. Geological Soc. Am. Bull. 198, 1608–1625.
Mellere, D., 1993. Thrust-generated, back-fill stacking of alluvial fan sequences, south-central Pyrenees, Spain (La Pobla de Segur Conglomerates). In: Frostick, L.E., Steel, R.J. (Eds.), Tectonic Controls and Signatures in Sedimentary Successions, volume 20. Special Publication of the International Association of Sedimentologists, pp. 259–276.
Metcalf, J.R., Fitzgerald, P.G., Baldwin, S.L., Muñoz, J.-A., 2009. Thermochronology of a convergent orogen: constraints on the timing of thrust faulting and subsequent exhumation of the Maladeta Pluton in the Central Pyrenean Axial Zone. Earth Planetary Sci. Lett. 287, 488–503.
Milliman, J.D., Syvitski, J.P.M., 1992. Geomorphic/tectonic control of sediment discharge to the ocean: the importance of small mountainous rivers. J. Geology 100, 525–544.
Muñoz, J.A., 1992. Evolution of a continental collision belt: ECORS-Pyrenees crustal balanced section. In: McClay, K.R. (Ed.), Thrust Tectonics. Chapman and Hall, London, pp. 235–246.
O'Sullivan, P.B., Parrish, R.R., 1995. The importance of apatite composition and single-grain ages when interpreting fission track data from plutonic rocks: a case study from the Coast Ranges. BC Earth Planetary Sci. Lett. 132, 213–224.
Puigdefàbregas, C., Muñoz, J.A., Vergés, J., 1992. Thrusting and foreland basin evolution in the Southern Pyrenees. In: McClay, K. (Ed.), Thrust Tectonics. Chapman and Hall, London, pp. 247–254.
Puigdefàbregas, C., Souquet, P., 1986. Tectonosedimentary cycles and depositional sequences of the Mesozoic and Tertiary from the Pyrenees. Tectonophysics 129, 173–203.
Rahl, J.M., Ehlers, T.A., van der Pluijm, B.A., 2007. Quantifying transient erosion of orogens with detrital thermochronology from syntectonic basin deposits. Earth Planetary Sci. Lett. 256, 147–161.
Rahl, J.M., Reiners, P.W., Campbell, I.H., Nicolescu, S., Allen, C.M., 2003. Combined single-grain (U–Th)/He and U/Pb dating of detrital zircons from the Navajo Sandstone. Utah: Geology Boulder 31, 761–764.
Reiners, P.W., Brandon, M.T., 2006. Using thermochronology to understand orogenic erosion. Annual Rev. Earth Planetary Sci. 34, 419–466.
Reynolds, R.C., 1993a. Three-dimensional powder X-ray diffraction from disordered illite: simulation and interpretation of the diffraction patterns. In: Reynolds, R.C., Walker, J.R. (Eds.), Computer Applications to X-Ray Powder Diffraction Analysis of Clay Minerals, volume 5. The Clay Minerals Society, CMS Workshop Lectures, Aurora, Colorado, pp. 43–78.
Reynolds, R.C., 1993b. WILDFIRE©: A computer program for the calculation of three-dimensional X-ray diffraction patterns for mica polytypes and their disordered variations. Reynolds, Hanover, New Hampshire. (lab manual).
Roe, G.H., Stolar, D.B., Willett, S.D., 2006. Response of a steady-state critical wedge orogen to changes in climate and tectonic forcing. In: Willett, S.D., Hovius, N., Brandon, M.T., Fisher, D.M. (Eds.), Tectonics, Climate, and Landscape Evolution, volume 398. Geological Society of America Special Paper, pp. 227–239.
Saura, L., 2004, Anàlisi estructural de la zona de los Nogueres [Ph.D. Thesis thesis].
Saura, L., Teixell, A., 2000. Relación entre los conglomerados oligocenos y las estructuras tectónicas en la Zona de les Nogureres, Pireneo central. Geotemas 2, 201–203.

Saura, L., Teixell, A., 2006. Inversion of small basins — effects of structural variations at the leading edge of the axial zone antiformal stack (southern Pyrenees, Spain). J. Struct. Geology 28, 1909–1920.
Seguret, M., Daignieres, M., 1986. Crustal scale balanced cross-sections of the Pyrenees: discussion. Tectonophysics 129, 303–318.
Simo, A., 1986. Carbonate platform depositional sequences, upper Cretaceous, south-central Pyrenees (Spain). Tectonophysics 129, 205–231.
Sinclair, H.D., Gibson, M., Naylor, M., Morris, R.G., 2005. Asymmetric growth of the Pyrenees revealed through measurement and modeling of orogenic fluxes. Am. J. Sci. 305, 369–406.
Solum, J.G., van der Pluijm, B., Peacor, D.R., 2005. Neocrystallization, fabrics and age of clay minerals from the Moab Fault. Utah: J. Struct. Geology 27, 1563–1576.
Souriau, A., Granet, M., 1995. A tomographic study of the lithosphere beneath the Pyrenees from local and teleseismic data. J. Geophysical Res. 100, 18117–18134.
Srodon, J., Eberl, D.D., 1984. Illite. In: Bailey, S.W. (Ed.), Reviews in Mineralogy. Mineralogical Society of America, Washington, D.C, pp. 495–544.
Stolar, D.B., Willett, S.D., Roe, G.H., 2006. Climatic and tectonic forcing of a critical orogen. In: Willett, S.D., Hovius, N., Brandon, M.T., Fisher, D.M. (Eds.), Tectonics, Climate, and Landscape Evolution, volume 398. Geological Society of America Special Paper, pp. 241–250.
Sussman, A., Butler, R., Dinarès-Turell, J., Vergés, J., 2004. Vertical-axis rotation of a foreland fold and implications for orogenic curvature: an example from the Southern Pyrenees, Spain. Earth Planetary Sci. Lett. 218, 435–449.
Tagami, T., O'Sullivan, P.B., 2005. Fundamentals of fission-track thermochronology. Rev. Mineralogy Geochemistry 58, 19–47.
van der Pluijm, B.A., Hall, C.M., Vrolijk, P.J., Pevear, D.R., Covey, M.C., 2001. The dating of shallow faults in the Earth's crust. Nature (London) 412, 172–175.
van der Pluijm, B.A., Vrolijk, P.J., Pevear, D.R., Hall, C.M., Solum, J.G., 2006. Fault dating in the Canadian Rocky Mountains: evidence for late Cretaceous and early Eocene orogenic pulses. Geology 34, 837–840.
van Lith, J.G.J., 1965. Geology of the Spanish part of the Gavarnie Nappe (Pyrenees) and its underlying sediments near Bielsa (Province of Huesca). Geologica Ultrajectina 10.
Vergés, J., Fernàndez, M., Martínez, A., 2002. The Pyrenean orogen; pre-, syn-, and post-collisional evolution. J. Virtual Explorer 8, 57–76.
Vermeesch, P., 2009. RadialPlotter: a Java application for fission track, luminescence and other radial plots. Radiat. Meas. 44, 409–410.
Vincent, S.J., 2001. The Sis palaeovalley: a record of proximal fluvial sedimentation and drainage basin development in response to Pyrenean mountain building. Sedimentology 48, 1235–1276.
Vincent, S.J., Elliott, T., 1997. Long-lived transfer zone paleovalleys in mountain belts: an example from the Tertiary of the Spanish Pyrenees. J. Sedimentary Res. 67, 303–310.
Vrolijk, P., van der Pluijm, B.A., 1999. Clay gouge. J. Struct. Geology 21, 1039–1048.
Whipple, K.X., Meade, B.J., 2004. Controls on the strength of coupling among climate, erosion, and deformation in two-sided, frictional orogenic wedges at steady state. J. Geophysical Res. 109.
Willett, S., 1999. Orogeny and orography: the effects of erosion on the structure of mountain belts. J. Geophysical Res. 104, 28957–28981.
Williams, E.A., Ford, M., Vergés, J., Artoni, A., 1998. Alluvial gravel sedimentation in a contractional growth fold setting, Saint Lorenc de Morunys, southeastern Pyrenees. In: Mascle, A., Puigdefàbregas, C., Luterbacher, H.P., Fernàndez, M. (Eds.), Cenozoic Foreland Basins of Western Europe, volume 134. Geological Society of London Special Publication, London, pp. 69–106.
Williams, G., 1985. Thrust tectonics in the south central Pyrenees. J. Struct. Geology 7, 11–17.
Ylagan, R., Kim, C., Pevear, D., Vrolijk, P., 2002. Illite polytype quantification for accurate K–Ar determination. Am. Mineralogist 87, 1536–1545.
Zwart, H.J., 1986. The Variscan geology of the Pyrenees. Tectonophysics 129, 9–27.